XANTHENE DYES-MEDIATED *IN VITRO* PHOTODYNAMIC TREATMENT OF CANCER AND NON-CANCER CELL LINES

Lukáš Malina[1,2], Kateřina Bartoň Tománková[1,2], Barbora Hošíková[1], Jana Jiravová[1,2], Jakub Hošík[1], Jana Zapletalová[1], Hana Kolářová[1]

[1]Department of Medical Biophysics, Faculty of Medicine and Dentistry, Palacky University in Olomouc, Czech Republic

[2]Institute of Molecular and Translational Medicine, Faculty of Medicine and Dentistry, Palacky University in Olomouc, Czech Republic

Abstract

Rose bengal and erythrosin B are xanthene dyes mainly known and used as antimicrobial agents, but due to their photodynamic activity they are also potential photosensitizers for cancer photodynamic therapy. The aim of this work is to study a photodynamic efficacy of rose bengal and erythrosin B against human skin melanoma and mouse fibroblast cell lines, compare them with each other and find out their photodynamic properties induced by light emitting diodes with total light dose of 5 J/cm^2. To fully identify and understand photodynamic properties of both potentially effective photosensitizers, a set of complex in vitro tests such as cell cytotoxic assay, measurement of reactive oxygen species production, mitochondrial membrane potential change assay, mode of cell death determination or comet assay were made. Although both photosensitizers proved to have similar properties such as increasing production of reactive oxygen species with the higher concentration, predominance of necrotic mode of death or genotoxicity, the more effective photosensitizer was rose bengal because its EC50 was over 20 times lower for both cell lines than in case of erythrosine B.

Keywords

photodynamic therapy; rose bengal; erythrosin B; reactive oxygen species; cytotoxicity

Introduction

Photodynamic therapy (PDT) is a photochemical-based treatment approach that involves the use of a combination of light and a light-activated chemical, called a photosensitizer [1]. Generally, PDT requires three essential components for the biochemical process to proceed: a photosensitizer, an appropriate light source and tissue oxygen [2].

The photosensitizer (PS) is light sensitive agent. Its administration can be systemic or topical depending mainly on the location of the cancer and also on the size of treated area. The PS molecule is a singlet in its ground state (it has two electrons with opposite spins) and the absorption of a photon with the appropriate quantum energy (wavelength) leads to the excitation of one electron into a higher-energy orbital [3]. This excited singlet state is short-lived (nanoseconds) and can lose its energy by emitting light (fluorescence) or by internal conversion into heat. The fact that most PS are fluorescent has led to the development of sensitive assays to quantify the amount of PS in cells or tissues and allows in vivo fluorescence imaging [4]. The excited single state PS can also convert into the triplet state via intersystem crossing and interact with surrounding molecules and thus produce reactive oxygen species (ROS) [5].

Each PS has an appropriate and optimal wavelength and intensity (fluence) of light for activation. Indeed, due to their structures many PS have several wavelengths that can lead to the photodynamic reaction [6]. There are three main classes of PDT light sources – lamps, LED and lasers. LED has become a viable technology for PDT in the last few years, particularly for irradiation of easily accessible tissue surfaces [7]. To minimize the absorption by endogenous chromophores and reduce the undesired photodamage of a healthy tissue, lasers with a narrow bandwidth, which have a well-controlled and focused output, are commonly used for PDT treatment. The output laser light can be delivered by optical fibres for the localized application [8].

ROS is a collective term that includes oxygen radicals and also some non-radical derivates of O_2 like H_2O_2, hypochlorous acid (HOCl), peroxynitrite

Lekar a technika – Clinician and Technology 2020, vol. 50(3), pp. 114–121, DOI: 10.14311/CTJ.2020.3.05
ISSN 0301-5491 (Print), ISSN 2336-5552 (Online)

($ONOO^-$), O_3 and singlet oxygen. Excited PS can produce ROS via two pathways—Type I and Type II [9]. In a Type I reaction, the PS in triplet state can directly react with a substrate and undergo an electron transfer reaction initially producing free radicals that may further react with oxygen to produce ROS (including hydroxyl radicals) [10]. However, most PSs are proposed to act through Type II reactions where singlet oxygen is the main molecule causing oxidative cellular damage [11]. Highly reactive oxygen species cause the photodamage of proteins, fats and other molecules in the photosensitized area [12]. Since ROS and singlet oxygen species have a high reactivity and short half-life, within PDT applications only those biological substrates that are close to the tumour region (where these cytotoxic species are generated) are directly affected and so healthy surrounding tissues generally remained unharmed [13].

Material and methods

Photodynamic treatment

Cell density for G361 (ATCC) and NIH3T3 (ATCC) cell lines was 10^4 per well and both cell lines were single layer. G361 and NIH3T3 cells were incubated in a thermobox at 37 °C and in 5% CO_2 for 24 h in 96-well plates with 100 µl of fresh DMEM medium. In experiments, the concentration ranges of rose bengal (RB) (Sigma) and erythrosin B (erB) (Sigma) were ½ EC50, EC50 and 2×EC50 excluding MTT assay where the ranges were 0.5–5 µM for RB/G361+NIH3T3 cell lines, 5–60 µM for erB/G361 cell line and 30–90 µM for erB/NIH3T3 cell line. The cells were then incubated in a thermobox at 37 °C and in 5% CO_2 for 24 h. Both cell lines were then exposed to a total irradiation dose of 5 J/cm^2 in 100 µl of PBS 1× with 5 mM glucose. For the irradiation we used a patented LED based light source (patent number: CZ 28377) specifically designed for the irradiation of experimental microplate with a peak emission wavelength of 525 nm, a spectral width of 35 nm and a light intensity set to 14,7 mW/cm^2. There were no significant changes of temperature during irradiation. The time needed for the stated total dose was 340 sec (5 J/cm^2). After irradiation we added fresh DMEM medium instead of PBS 1× and cultivated cells in a thermobox under the same conditions for 24 h. All assays were performed in three independent measurements and each in triplicates. As the control we used cells with light irradiation and no PS.

Cell cytotoxic assay (MTT)

The cell cytotoxic effect and EC50 on the G361 and NIH3T3 cells were determined using the MTT assay. After 24 h of incubation after the treatment we added 50 µl of MTT (Sigma) dissolved in PBS 1× and incubated the cells for another 3 h at 37 °C and in 5% CO_2. The solution was then carefully replaced with 100 µl of DMSO (Sigma) in order to solubilize the violet formazan crystals. The measurement of absorbance was carried out on a Synergy HT multi-mode microplate reader (BioTek, USA) at 570 nm and 690 nm. The cell viability of the samples was determined as a percentage of the control cell viability (100×average of test group/average of control group). Using the Phototox v. 2.0 software (ZEBET, Germany) data were calculated for the determination of EC50.

To verify there is no cytotoxic effect in case of either both substances or green light, the MTT assay was performed.

Measurement of reactive oxygen species production

ROS detection during PDT was performed by using a CM-H_2DCFDA (Invitrogen) solution (10 µl 10 µM DCF + 1 ml PBS) and a microplate reader Synergy HT. Right after adding 50 µl of DCF solution, 25 min incubation and irradiation, the ROS kinetic production was determined during 10 min intervals. An excitation wavelength of 485 nm and an emission wavelength of 548 nm were used. Results are presented as a linear regression coefficient. The regression coefficient was calculated using function SLOPE in MS Excel from the linear part of curves.

Mitochondrial membrane potential change assay

Mitochondrial membrane potential change (MMP) was monitored by the fluorescent dye JC 1 (Sigma). After the 24 h incubation cells were washed by PBS 1×. Then 50 µl of a JC-1 solution was added (5 mg/ml in DMSO + 5 ml PBS 1×) and cells were incubated at 37 °C and in 5% CO_2 for 20 min. Afterwards incubation cells were washed by PBS 1× twice and then the green and red fluorescence was measured by Synergy HT reader. The results were expressed as the ratio of the green fluorescence (excitation wavelength: 485 nm, emission wavelength: 548 nm) and red fluorescence (excitation wavelength: 520 nm, emission wavelength: 590 nm) retained within the cells.

Detection of apoptotic and necrotic cells

After PDT cells were washed by PBS 1× and 50 µl of annexin FITC apoptosis detection kit solution (Sigma) was added. The kit consisted of annexin V-FITC, propidium iodide, binding buffer and distilled water. After kit application the cells were incubated for 10 min at 37 °C and in 5% CO_2. Generally, a phosphatidylserine is in the inner part of the lipid double-layer, but when the apoptosis begins, the phosphatidylserine is moved to the outer part of the lipid double-layer and

Lekar a technika – Clinician and Technology 2020, vol. 50(3), pp. 114–121, DOI: 10.14311/CTJ.2020.3.05
ISSN 0301-5491 (Print), ISSN 2336-5552 (Online)

is accessible to annexin (green signal). In case of necrosis, the nuclear membrane is severely damaged and the propidium iodide is able to attach to the DNA (red signal). Using a fluorescence microscope Olympus IX81 with DSU unit (Olympus, Japan), the fluorescence signals of the cells were manually scored and determined as a percentage of the total number of cells.

Comet assay

To begin we precoated microscope slides with 1% HMP agarose (Serva) dissolved in distilled water. After stiffening we made two 1% agarose spots (dissolved in PBS 1×) and overlay them with a cover slip. The G361 and NIH3T3 cells were after PDT trypsinized, rinsed by DMEM, shifted into tubes and centrifuged (2 min, 1500 rpm). The mixture of 25 µl of cell suspension and 85 µl of 1% LMP agarose (Qbiogene) dissolved in PBS 1× was added to the microscope slides with agarose gel. The microscope slides were immersed in a lysis buffer with 1% Triton X (Serva) for 1 h and then placed in an electrophoretic tank and dipped into a cool electrophoresis solution for 40 min. The settings of electrophoresis were 20 V and 350 mA for 20 min. Afterwards the electrophoresis, the microscopic slides were immersed in a neutralisation buffer (10 min twice). The samples were then stained by SYBR Green (Invitrogen) for 15 min and scored by the SW Comet Score (TriTek Corp., USA).

Statistical analysis

The results were processed using the software Statistica v.13. The data sets are from three independent experiments. To analyse data sets the ANOVA with post hoc tests, Student's t-test and Bonferroni correction were used. All concentrations were compared with a relevant control group.

Results

The MTT assay proved no statistically significant cytotoxicity in case of either both PSs or green light. The MTT viability test results of RB and erB after PDT in Fig. 1 show expected tendency—the higher concentration of PS the lower viability of cells. This was proved for both cell lines and PSs.

These results were then converted into EC50 by Phototox version 2.0 and they are presented in Table 1 together with calculated $^1/_2$ EC50 and 2×EC50 which were then used as the concentration ranges in following experiments.

A comparison between both cell lines shows that values of G361 were more than 2 times lower than the values of the NIH3T3. This fact indicates higher accumulation in tumorous G361 cells. A comparison of both PSs shows significantly lower EC50 of RB for both cell lines. According to our results, the value of EC50 is over 20 times lower than in case of erB which makes RB more effective.

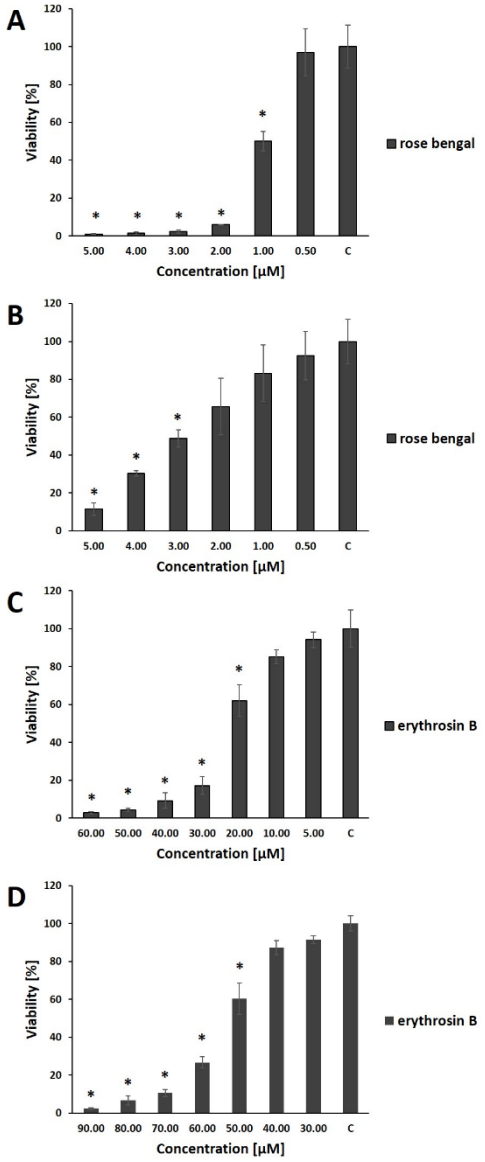

Fig. 1: The dependence of G361 and NIH3T3 cell viability on the concentration of RB and erB. The total irradiation dose used was 5 J/cm^2 (total irradiation time was 340 seconds and intensity of radiation was 14,7 mW/cm^2). The control represents irradiated cells without PS and its value was set as 100%. A – RB + G361 cell line; B – RB + NIH3T3 cell line; C – erB + G361 cell line; D – erB + NIH3T3 cell line. Data represent the mean and standard error from three independent measurements and each in triplicates.
** RB: p<0.014, statistically different compared with control (C)*
** erB: p<0.01, statistically different compared with control (C).*

Lekar a technika – Clinician and Technology 2020, vol. 50(3), pp. 114–121, DOI: 10.14311/CTJ.2020.3.05
ISSN 0301-5491 (Print), ISSN 2336-5552 (Online)

Table 1: EC50 and calculated $^1/_2$ EC50 and 2×EC50 of G361 and NIH3T3 cell lines.

PS	Cell line	$^1/_2$ EC50 (μM)	EC50 (μM)	2×EC50 (μM)
RB	G361	0.50	* 1.01±0.03	2.01
RB	NIH3T3	1.45	* 2.90±0.15	5.80
erB	G361	11.19	+ 22.37±0.39	44.75
erB	NIH3T3	26.96	+ 53.92±0.66	107.85

Notes: EC50 were determined by Phototox version 2.0 software. Data represent the mean and standard error from three independent measurements and each in triplicates.
*: p<0.0001, EC50 of both cell lines are statistically different compared with each other
+: p<0.0001, EC50 of both cell lines are statistically different compared with each other

To find out and potentially prove toxic effect of PSs we used the kinetic detection of ROS and measured values for 10 minutes right after irradiation. The kinetic results were then converted into linear regression coefficient. The higher this coefficient is the more ROS was detected in each minute. The Fig. 2 shows dependence of ROS on the concentration of PS—the higher concentration the more ROS was produced. The erB seems to cause no significant difference in amount of ROS between both cell lines which is in contrary to the RB. Although there is a big difference in concentrations of RB and erB, the differences in amount of ROS are not as big as might be expected.

To evaluate the changes of MMP (typical for the early phase of apoptosis) in cells after PDT we used MMP change assay. When the cells are undamaged, the red fluorescent aggregates of JC-1 are formed in the mitochondrial matrix due to the MMP. However, when the MMP of cells is lost, the JC-1 probe forms green monomers. The changes of MMP are determined by the median proportion of green and red fluorescence. The higher the value of the median proportion, the higher rate of dysfunction of the mitochondria and higher probability of early phase of apoptosis. The results of both PSs (Fig. 3) show similar trend in both cell lines. The higher the concentration of PS, the higher increase of value in comparison with the control. The exception in both cases was the highest concentration where the value suddenly decreased.

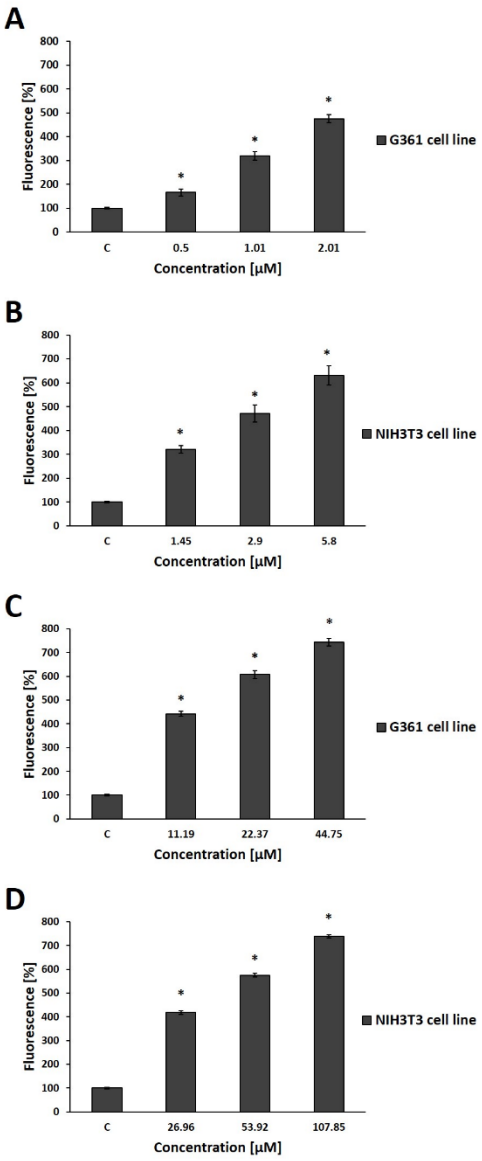

Fig. 2: Percentage increase of ROS in concentration of $^1/_2$ EC50, EC50, 2×EC50 and total radial dose of 5 J/cm^2. The control represents irradiated cells without PS. A – RB+G361 cell line; B – RB+NIH3T3 cell line; C – erB+G361 cell line; D – erB+NIH3T3 cell line. Data represent the mean and standard error from three independent measurements and each in triplicates. Notes: The linear regression of ROS rate expressed the ROS amount created at each minute.
**: p<0.0001, statistically different compared with control (C).*

To distinguish two types of death the cell can undergo we used Annexin FITC apoptosis detection kit and established ratio [%] between apoptotic and necrotic cells. The results presented in Fig. 4 show that in case of both PSs and cell lines the necrotic cells predominate

Lekar a technika – Clinician and Technology 2020, vol. 50(3), pp. 114–121, DOI: 10.14311/CTJ.2020.3.05
ISSN 0301-5491 (Print), ISSN 2336-5552 (Online)

even in the lowest concentration. The results of mode of death ratio proved PS concentration dependency—the higher concentration of PS the more cells underwent necrosis.

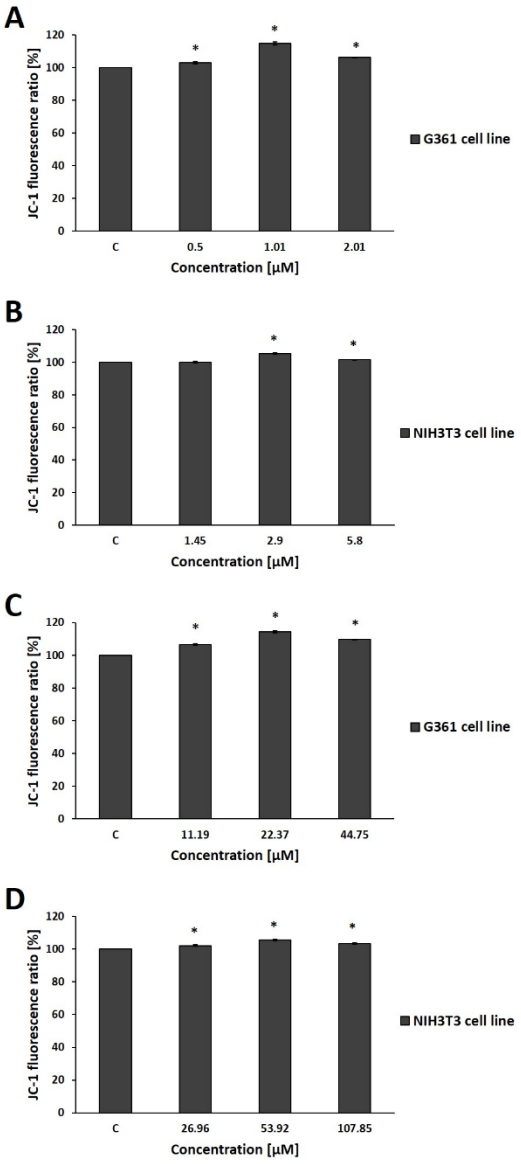

Fig. 3: The dependence of MMP changes in G361 and NIH3T3 cell lines on the concentration of ½ EC50, EC50 and 2×EC50 and total radial dose of 5 J/cm². The control represents irradiated cells without PS. A – RB+G361 cell line; B – RB+NIH3T3 cell line; C – erB+G361 cell line; D – erB+NIH3T3 cell line. Data represent the mean and standard error from three independent measurements and each in triplicates. Notes: The higher the fluorescence ratio, the greater the cell damage.
**: p<0.009, statistically different compared with control (C).*

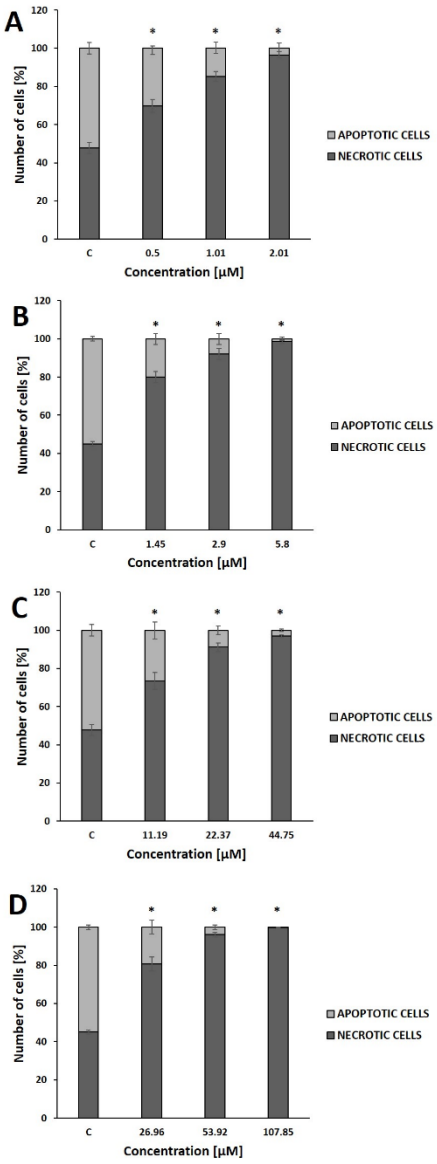

Fig. 4: Apoptotic and necrotic cells ratio in G361 and NIH3T3 cell lines, the concentration of of ½ EC50, EC50 and 2×EC50 and total radial dose of 5 J/cm². The control represents irradiated cells without PS. A – RB+G361 cell line; B – RB+NIH3T3 cell line; C – erB+G361 cell line; D – erB+NIH3T3 cell line. Data represent the mean and standard error from three independent measurements and each in triplicates.
**: p<0.0066, statistically different compared with control (C).*

The genotoxicity of PSs can be determined by comet assay via fragmentation of DNA after PDT. The quantity of DNA in head and tail of comet is shown in Fig. 5. In low concentration of both PSs the majority of DNA still remained in the head of comet, thus they caused almost no DNA fragmentation. On the other hand, the

Lekar a technika – Clinician and Technology 2020, vol. 50(3), pp. 114–121, DOI: 10.14311/CTJ.2020.3.05
ISSN 0301-5491 (Print), ISSN 2336-5552 (Online)

higher the concentration, the more DNA in the comet tail and the greater DNA fragmentation. This fact indicates the genotoxicity of both PSs in both cell lines. In comparison between both PSs the erB seems to be generally a little bit more genotoxic than RB, but it's also important to take into consideration the fact that the concentration of erB is over 20 times higher than RB.

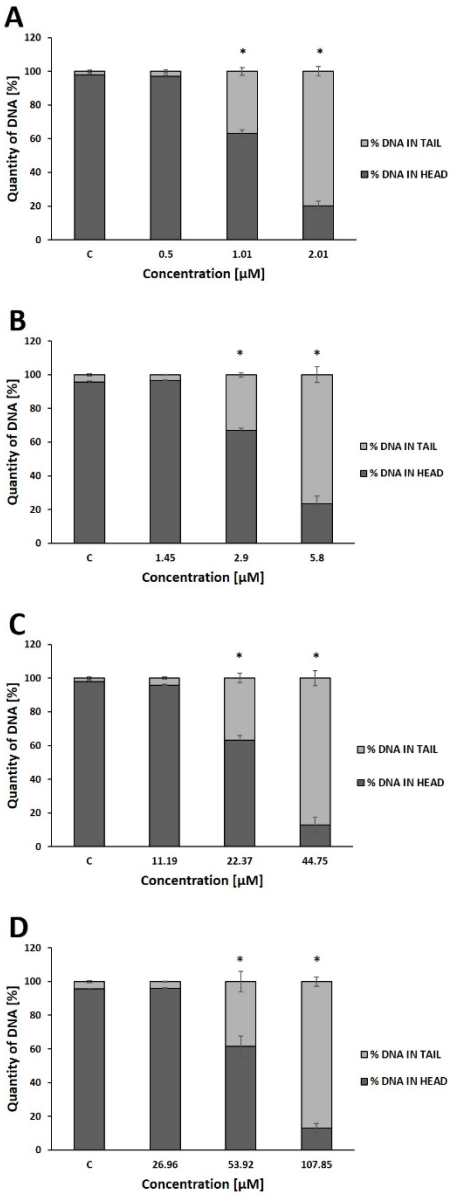

Fig. 5: Quantity of DNA in the tail and in the head determined by comet assay for G361 and NIH3T3 cell lines, the concentration of of ½ EC50, EC50 and 2×EC50 and total radial dose of 5 J/cm². The control represents irradiated cells without PS. A – RB+G361 cell line; B – RB+NIH3T3 cell line; C – erB+G361 cell line; D – erB+NIH3T3 cell line. Data represent the mean and standard error from three independent measurements and each in triplicates.
**: p<0.004, statistically different compared with control (C).*

Discussion

One of the most wanted properties of PS is no toxicity without irradiation. Thus, we tested cytotoxicity of the RB and erB to evaluate their influence on the viability of tested cells. Dark toxicity test (PS with no irradiation) proved no cell destruction and thus no toxicity of both PSs without light which corresponds with the results of other researches such as Dabrzalska et al. [14]. Previous experiments also proved no cell destruction using only green light with no PS.

The MTT viability test shows higher efficacy of RB in comparison to erB. This result is supported by Buck et al. [15]. Their research was focused on photodynamic efficacy and phototoxicity of the xanthene dyes (including RB and erB) against a carcinoma cell line (larynx carcinoma). Although they used different wavelength and light dose, the results seem to be similar and RB was several times more effective than erB.

McEwan et al. [16] investigated the relative efficacy of PDT for the treatment of cancer. Their results, as well as ours, proved RB to be effective as PS in PDT against cancer cells. The difference in viability between both studies is probably due to different cancer cell lines (RIF 1, HeLa and B16), light source and light dose.

In contrast to cancer PDT, there are many studies focused on antimicrobial photodynamic therapy (aPDT) mediated by RB and erB. Rossoni et al. [17] compared the efficacy of both PSs against Enterobacteriaceae. Their results of efficacy of RB and erB in case of aPDT were the same as our PDT as the RB proved to be much more effective in comparison to erB.

Calori et al. [18] studied the membrane penetration of xanthene dyes to find out the best candidate for photodynamic action. According to their work the RB seems to penetrate membrane more easily than erB. The membrane penetration may affect the concentration of PS added to cells and may also be one of the reasons why EC50 of the RB is much lower than EC50 of erB and thus why RB is more effective.

The low effective concentration is desired because it decreases the probability of some undesirable effects such as photosensitivity. The dependency of skin photosensitivity to PS dose is stated in several studies such as Kniebühler et al. [19] or Wang et al. [20].

The results of ROS production show the dependence on concentration – the higher concentration the higher ROS production. This concentration-dependent manner was also observed by Srivastav et al. [21] in their study on A375 cell line. Despite the fact that the concentration of RB was over 20 times lower than the concentration of erB, the difference in amount of ROS was not as big as we would assume, especially in case of G361 cell line. This fact indicates higher ROS production of RB in comparison with erB which is supported by several studies such as Pellosi et al. [22].

Lekar a technika – Clinician and Technology 2020, vol. 50(3), pp. 114–121, DOI: 10.14311/CTJ.2020.3.05
ISSN 0301-5491 (Print), ISSN 2336-5552 (Online)

Results of RB-mediated ROS generation made by Song et al. [23] on Cal27 cell line showed significant increase of ROS level (up to threefold higher) when compared to control cells. This increment is comparable with our results of ROS and proves ability of RB to increase production of cytotoxic ROS in cancer cells.

Although the study showed the higher concentration the higher the probability of early phase of apoptosis, it applies only until the concentration is too cytotoxic and cause more cells underwent necrosis. Rabe et al. [24] studied RB and early phase of apoptosis on NIH3T3 and AGS cell lines. Although the conditions were different, the trend and sudden decrease of early phase of apoptosis corresponds with the study.

As Liu et al. [25] stated, the ROS can cause DNA base oxidative damage, strand breaks and cross-links, although compared with ionizing radiation, the PDT-induced DNA damage seems nonlethal. Our results of comet assays showed that both PSs caused oxidative damage of DNA. The combination of ROS production and comet assay results indicates the higher concentration of PS the higher ROS production and higher DNA damage. Comet assay in our study showed the gradual increase in DNA damage as the concentration of RB increased. The similar DNA damage dependency on concentration of RB in case of A375 cell line also reported Srivastav et al. [21].

Garg et al. [26] stated that necrosis usually predominates when using high dose PDT whereas apoptosis is more usually seen with comparatively lower PDT doses. High doses in PDT include high concentration of PS or/and high light doses. Our results of apoptotic and necrotic cell death ratio proved the statement as the percentage of necrotic cells predominates more with the higher concentration of RB and erB. The predominance of necrosis may also be influenced by properties of PSs. Both RB and erB are hydrophilic dyes and thus they are taken up by pinocytosis and localize preferentially in extranuclear granules, mainly lysosomes [27]. The PDT damage of lysosomes then releases the proteolytic enzymes and leads to necrosis.

Conclusion

Rose bengal and erythrosin B are xanthene dyes with great antimicrobial properties studied by many researchers. This work is focused on demonstrating their photodynamic and anticancer properties which make them to be potentially very effective PSs in PDT. The study compares the PSs in various concentrations on G361 and NIH3T3 cell lines. According to our results of EC50, the most effective PS seems to be RB. Its half maximal effective concentration is over 20 times lower in comparison with erB. Subsequent tests demonstrated other properties of both PSs such as ROS production, changes of $\Delta\Psi m$, genotoxicity or mode of death. Although xanthene dyes are mostly known in connection with aPDT, the anticancer PDT using xanthene dyes is not examined as in case of other usually studied PSs such as ALA, methylene blue, porphyrins or phthalocyanines. This study was focused on PDT on cancer and non-cancer cell lines and helped find out the fundamental properties of these potentially very effective PSs.

Acknowledgement

This work has been supported by the European Regional Development Fund - Project ENOCH (No. CZ.02.1.01/0.0/0.0/16_019/0000868) and IGA_LF_2020_015.

References

[1] Li X, Lee S, Yoon J. Supramolecular photosensitizers rejuvenate photodynamic therapy. Chemical Society Reviews. 2018;47(4):1174–88. DOI: 10.1039/C7CS00594F

[2] Kim M, Jung HY, Park HJ. Topical PDT in the treatment of benign skin diseases: principles and new applications. International journal of molecular sciences. 2015;16:23259–78. DOI: 10.3390/ijms161023259

[3] Abrahamse H, Hamblin MR. New photosensitizers for photodynamic therapy. Biochemical Journal. 2016;473(4):347–64. DOI: 10.1042/BJ20150942

[4] Bayona AM, Mroz P, Thunshelle C, Hamblin MR. Design features for optimization of tetrapyrrole macrocycles as antimicrobial and anticancer photosensitizers. Chemical biology and drug design. 2017;89(2):192–206. DOI: 10.1111/cbdd.12792

[5] Hong EJ, Choi DG, Shim MS. Targeted and effective photodynamic therapy for cancer using functionalized nanomaterials. Acta Pharmaceutica Sinica B. 2016;6(4):297–307. DOI: 10.1016/j.apsb.2016.01.007

[6] Allison RR, Moghissi K. Oncologic photodynamic therapy: Clinical strategies that modulate mechanisms of action. Photodiagnosis and photodynamic therapy. 2013;10(4):331–41. DOI: 10.1016/j.pdpdt.2013.03.011

[7] Nagata JY, Hioka N, Kimura E, Batistela VR, Terada RS, Graciano AX, et al. Antibacterial photodynamic therapy for dental caries: Evaluation of the photosensitizers used and light source properties. Photodiagnosis and photodynamic therapy. 2012;9(2):122–31. DOI: 10.1016/j.pdpdt.2011.11.006

[8] Qiu H, Tan M, Ohulchanskyy TY, Lovell JF, Chen G. Recent Progress in Upconversion Photodynamic Therapy. Nanomaterials. 2018;8(5):344. DOI: 10.3390/nano8050344

[9] Rajendran M. Quinones as photosensitizer for photodynamic therapy: ROS generation, mechanism and detection methods. Photodiagnosis and photodynamic therapy. 2016;13:175–87. DOI: 10.1016/j.pdpdt.2015.07.177

[10] Wen X, Li Y, Hamblin MR. Photodynamic therapy in dermatology beyond non-melanoma cancer: An update. Photodiagnosis and photodynamic therapy. 2017;19:140–52. DOI: 10.1016/j.pdpdt.2017.06.010

[11] Meng Z, Hou W, Zhou H, Zhou L, Chen H, Wu C. Therapeutic Considerations and Conjugated Polymer-Based Photosensitizers for Photodynamic Therapy. Macromolecular Rapid Communications. 2017;39(5). DOI: 10.1002/marc.201700614

[12] Kwiatkowski S, Knap B, Przystupski D, Saczko J, Kedzierska E, Knap-Czop K, et al. Photodynamic therapy – mechanisms, photosensitizers and combinations. Biomedicine and Pharmacotherapy. 2018;106:1098–1107. DOI: 10.1016/j.biopha.2018.07.049

[13] Mokwena MG, Kruger CA, Ivan MT, Heidi A. A review of nanoparticle photosensitizer drug delivery uptake systems for photodynamic treatment of lung cancer. Photodiagnosis and photodynamic therapy. 2018;22:147–54. DOI: 10.1016/j.pdpdt.2018.03.006

[14] Dabrzalska M, Janaszewska A, Zablocka M, Mignani S, Majoral JP, Klajnert-Maculewicz. Cationic Phosphorus Dendrimer Enhances Photodynamic Activity of Rose Bengal against Basal Cell Carcinoma Cell Lines. Molecular Pharmaceutics. 2017;14:1821–30. DOI: 10.1021/acs.molpharmaceut.7b00108

[15] Buck ST, Bettanin F, Orestes E, Homem-de-Mello P, Imasato H, Viana RB, et al. Photodynamic Efficiency of Xanthene Dyes and Their Phototoxicity against a Carcinoma Cell Line: A Computational and Experimental Study. Journal of Chemistry. 2017. DOI: 10.1155/2017/7365263

[16] McEwan C, Nesbitt H, Nicholas D, Kavanagh OS, McKenna K, Loan P, et al. Comparing the efficacy of photodynamic and sonodynamic therapy in non-melanoma and melanoma skin cancer. Bioorganic and Medicinal Chemistry. 2016;24(13): 3023–8. DOI: 10.1016/j.bmc.2016.05.015

[17] Rossoni RD, Junqueira JC, Santos EL, Costa AC, Jorge AO. Comparison of the efficacy of Rose Bengal and erythrosin in photodynamic therapy against Enterobacteriaceae. Lasers in Medical Science. 2010;25:581–6. DOI: 10.1007/s10103-010-0765-1

[18] Calori IR, Pellosi DS, Vanzin D, Cesar GB, Pereira PC, Politi MJ, et al. Distribution of Xanthene Dyes in DPPC Vesicles: Rationally Accounting for Drug Partitioning Using a Membrane Model. Journal of the Brazilian Chemical Society. 2016;27(11):1938–48. DOI: 10.5935/0103-5053.20160079

[19] Kniebühler G, Pongratz T, Betz CS, Göke B, Sroka R, Stepp H, Schirra J. Photodynamic therapy for cholangiocarcinoma using low dose mTHPC (Foscan). Photodiagnosis and photodynamic therapy. 2013;10:220–8. DOI: 10.1016/j.pdpdt.2012.12.005

[20] Wang Y, Lin Y, Zhang H, Zhu J. A photodynamic therapy combined with topical 5-aminolevulinic acid and systemic hematoporphyrin derivative is more efficient but less phototoxic for cancer. Journal of Cancer Research and Clinical Oncology. 2015;142(4):813–21. DOI: 10.1007/s00432-015-2066-3

[21] Srivastav AK, Mujtaba SF, Dwivedi A, Amar SK, Goyal S, Verma A, et al. Photosensitized rose Bengal-induced phototoxicity on human melanoma cell line under natural sunlight exposure. Journal of Photochemistry and Photobiology B: Biology. 2016;156:87–99. DOI: 10.1016/j.jphotobiol.2015.12.001

[22] Pellosi DS, Estevao BM, Semensato J, Severino D, Baptista MS, Politi MJ, et al. Photophysical properties and interactions of xanthene dyes in aqueous micelles. Journal of Photochemistry and Photobiology A: Chemistry. 2012;247:8–15. DOI: 10.1016/j.jphotochem.2012.07.009

[23] Song L, Li C, Zou Y, Dai F, Luo X, Wang B, et al. O_2 and Ca^{2+} Fluxes as Indicators of Apoptosis Induced by Rose Bengal–Mediated Photodynamic Therapy in Human Oral Squamous Carcinoma Cells. Photomedicine and Laser Surgery. 2015; 33(5):258–65. DOI: 10.1089/pho.2014.3863

[24] Rabe SZ, Mousavi SH, Tabasi N, Rastin M, Rabe SZ, Siadat Z, Mahmoudi M. Rose Bengal suppresses gastric cancer cell proliferation via apoptosis and inhibits nitric oxide formation in macrophages. Journal of Immunotoxicology. 2014;11(4):367–75. DOI: 10.3109/1547691X.2013.853715

[25] Liu Y, Meng X, Bu W. Upconversion-based photodynamic cancer therapy. Coordination Chemistry Reviews. 2019;379: 82–98. DOI: 10.1016/j.ccr.2017.09.006

[26] Garg AD, Bose M, Ahmed MI, Bonass WA, Wood SR. In Vitro Studies on Erythrosine-Based Photodynamic Therapy of Malignant and Pre-Malignant Oral Epithelial Cells. PLoS ONE. 2012;7(4):e34475. DOI: 10.1371/journal.pone.0034475

[27] Calzavara-Pinton PG, Venturini M, Sala R. Photodynamic therapy: update 2006 Part 1: Photochemistry and photobiology. Journal of the European Academy of Dermatology and Venereology. 2007;21(3):293–302. DOI: 10.1111/j.1468-3083.2006.01902.x

Lukáš Malina, MSc
Department of Medical Biophysics
Faculty of Medicine and Dentistry
Palacky University in Olomouc
Křížkovského 511/8, 771 47 Olomouc

E-mail: lukas.malina@upol.cz
Phone: +420 585 632 113